Nonlinear wake waves in a plasma and single cycle pulse generation

F. Pegoraro

International Workshop on Frontiers of Plasma Science, ICTP, Trieste August 2006

In collaboration with
S.S. Bulanov, S.V. Bulanov. T.Zh. Esirkepov

Dipartimento di Fisica Università di Pisa pegoraro@df.unipi.it

Overview

Present day laser technology allows us to generate ultraintense laser pulses with intensities approaching 10^{22} W/cm^2.

T. Tajima, G. Mourou, *Phys. Rev. ST Accel. Beams*, **5**, 031301 (2002).

In this regime the relativistic dynamics of the electrons in the plasma inside which the pulse propagates, introduces a *new type of nonlinear phenomena* that arise from the nonlinearity of the Lorentz force and of the relationship between particle momentum and velocity and, at very large intensities, from nonlinear quantum electrodynamics effects such as electron-positron pair creation.

These nonlinear processes can be harnessed in order to concentrate the e. m. radiation in space and in time and produce e.m. pulses of unprecedented high intensity or short duration that can be used to explore ultra-high energy density effects in plasmas : "*relativistic engineering*", as introduced in S.V. Bulanov, *et al.*, Phys. Rev. Lett. **91**, 085001 (2003).

See also:

S.V. Bulanov, *et al.*, in *Reviews of Plasma Physics*, ed. V.D. Shafranov, **22**, 227, Kluwer Acad., N.Y., (2001).
G.A. Mourou, *et al.*, *Rev, Mod. Phys.*,**78**, 309 (2006).
T. Esirkepov, *et al.*, *Phys. Rev. Lett.*, **92**, 175003 (2004).
S.V. Bulanov, *et al.*, *Plasma Phys. Rep.*, **30**, 196 (2004).
F. Pegoraro, *et al.*, *Phys. Lett. A*, **347**, 133 (2005).

One of these new possibilities was emphasized by the results presented in N.M. Naumova, $et\ al.$, Phys. Rev. Lett. **92**, 063902 (2004), where it is shown that synchronized attosecond ($10^{-18}\ sec$) e. m. pulses and attosecond electron bunches can be produced during the interaction of tightly focused, ultrashort laser pulses with overdense plasmas.

Similarly, the property of nonlinear systems to respond anharmonically to a periodic driving force was exploited in S.V. Bulanov, $et\ al.$, Phys. Rev. E **67**, (2003), where the propagation of a high intensity short laser pulse in a thin wall hollow channel was shown to produce a coherent ultrashort pulse with very short wavelength that propagates outwards through the channel walls.

A different method of generating ultra-short e. m. pulses was proposed in A.V. Isanin, *et al.*, Phys. Lett. **A 337**, 107 (2005).

This method uses the interaction between coherent nonlinear plasma structures (in particular a relativistic electromagnetic sub-cycle soliton) and the density modulations of a Langmuir wakefield in a plasma acting as a relativistic mirror.

In my two presentations I will illustrate this method taking time to review the theory of the elementary nonlinear plasma phenomena that are put to work in this approach: wake Langmuir waves, relativistic solitons and electron vortices.

Direct experimental visualization of atomic and electron dynamics with attosecond pulses,
Lin, C. D., Tong, X. M., Morishita, Toru,
Journal of Physics B: **39**, S419 (2006).

"We illustrate how attosecond light pulses can be used directly in mapping out the time dependence of the motion of atoms in a small molecule, as well as of the correlated motion of two excited electrons in an atom. For simple molecules such as H^2 and D^2, we show that the vibrational wave packet can be mapped out very accurately, including details due to the broadening and interference. For doubly excited states of a helium atom, we show that the time-dependent correlated motion between the two electrons can be mapped via double ionization with attosecond pulses."

Route to intense single attosecond pulses,
Tsakiris, G.D., Eidmann, K., Meyer-ter-Vehn, J., Krausz, F.,
New Journal of Physics,**8**, 19 (2006).

"A feasibility study is presented for the generation of single attosecond pulses using harmonics produced by planar targets irradiated at high intensities. The investigation focuses on the interaction of a few-optical cycles, carrier-envelope phase controlled, near-infrared laser pulse with an overdense plasma. The results obtained using an one-dimensional particle-in-cell code indicate that at laser intensities of $10^{20}\ W\ cm^{-2}$ a single sub-fs pulse can be generated in the $20 - 70\ eV$ spectral range with an efficiency of a few per cent and with 10^{-3} to 10^{-4} for higher photon energies."

Relativistic Mirrors

The reflection of an e.m. field structure from a moving mirror can be derived by performing a Lorentz transformation to the reference frame where the mirror is at rest.

In this frame the e.m. fields are Fourier transformed with respect to time and the appropriate (frequency dependent) reflection coefficient is used.

For a perfect mirror the standard condition that the tangential component on the electric field vanishes in the mirror frame is used.

The form and amplitude of the reflected pulse in the laboratory frame are then obtained by adding the reflected Fourier components and by performing the inverse Lorentz transformation of the resulting e.m. fields.

In the case on an electromagnetic wave. the frequency of the reflected wave is given in the laboratory frame by [1]

$$\omega_r = \omega_0 \frac{1 + 2\beta_M \cos\theta_0 + \beta_M^2}{1 - \beta_M^2} \tag{1}$$

where $\beta_M c$ is the mirror velocity and θ_0 is the incidence angle, while the reflection angle is given by

$$\cos\theta_r = \frac{(1 + \beta_M^2)\cos\theta_0 + 2\beta_M^2}{1 + \beta_M^2 + 2\beta_M \cos\theta_0} \tag{2}$$

The wave amplitude transforms according to $E_0/\omega_0 = E_r/\omega_r$.

[1] A. Einstein, *Ann. Phys.* (Leipzig) **17**, 891 (1905).
W. Pauli, in *Theory of Relativity*, Dover Publications, Inc., New York, (1981).

At normal incidence

$$\omega_r = \omega_0 \frac{(1 \pm \beta_M)^2}{1 - \beta_M^2} \tag{3}$$

i.e. for a co-propagating ($\beta_M > 0$) mirror (frequency downshift, the mirror gains energy from the wave)

$$\omega_r = \omega_0 \frac{1 + \beta_M}{1 - \beta_M} \sim 4/\gamma_M^2 \qquad \text{for} \quad \beta_M \to 1, \tag{4}$$

while for a counterpropagating mirror (frequency upshift, the mirror gives energy to the wave)

$$\omega_r = \omega_0 \frac{1 - \beta_M}{1 + \beta_M} \sim \gamma_M^2/4 \qquad \text{for} \quad \beta_M \to -1. \tag{5}$$

In the reflection the number of oscillations inside the e.m. wave is conserved.

How to construct a relativistic mirror

The mechanism envisaged is based on the results derived in S V. Bulanov, *et al.*, Phys. Rev. Lett. **91**, 085001 (2003), where it was shown, that when a laser pulse interacts with a *breaking wake plasma wave*, part of the pulse[2] is reflected in the form of a highly compressed and focused e. m. pulse with an up-shifted carrier frequency due to the Doppler effect.

The pulse enhancement of the pulse intensity and the pulse compression arise because the electron density modulations in the wake wave act as *parabolic relativistic mirrors*.

[2]The frequency dependent reflection coefficient $\rho(\omega') = -q/(q - i\omega'),$ is used. Here $q = 2\omega_{pe}(2\gamma_{ph})^{1/2}$ with γ_{ph} the Lorentz factor corresponding to the phase velocity of the wake wave that takes the place of γ_M in the previous formulae. This coefficient is obtained by solving the wave equation with a "foil current" linear in the vector potential

Breaking waves

Electromagnetic waves with relativistic amplitudes in underdense plasmas

Constant amplitude solutions of the equations for linear e.m. (transverse) and Langmuir (longitudinal) waves can be written in the form of waves propagating with constant velocity:

$$u(x,t) = u_t \cos[kx - (k^2c^2 + \omega_{\rm pe}^2)^{1/2}t]$$

$$\text{and} \qquad u(x,t) = u_l \cos[kx - \omega_{\rm pe}t)].$$

For finite amplitude waves the frequency depends on the wave amplitude.
In the theory of the interaction of high-intensity laser radiation with plasmas the paper A.I. Akhiezer R.V. Polovin, *Sov Phys. JETP* **30,** 915 (1956) has played a key role.

Maxwell's equations and cold collisionless plasma with ions at rest.

$$\Delta\mathbf{A} - \frac{1}{c^2}\partial_{\rm tt}\mathbf{A} - \frac{1}{c}\nabla\partial_{\rm t}\varphi - \frac{4\pi e n_e}{m_e c^2\gamma}(\mathcal{P} + \frac{e}{c}\mathbf{A}) = 0, \tag{6}$$

$$n_e = n_i(x) + \frac{1}{4\pi e}\Delta\varphi, \tag{7}$$

$$\partial_{\rm t}\mathcal{P} = \nabla(e\varphi - m_e c^2\gamma) + \frac{1}{\gamma}(\mathcal{P} + \frac{e}{c}\mathbf{A}) \times {\rm rot}\mathcal{P}. \tag{8}$$

The continuity equation is implied by equations (6,7). These equations are written in the Coulomb gauge:

$$\mathrm{div}\ \mathbf{A} = 0\,. \tag{9}$$

Here $\mathcal{P}$ is the canonical electron momentum, $\mathcal{P} = \mathbf{p} - e\mathbf{A}/c$, and the relativistic Lorentz factor is $\gamma = \left[1 + (\mathcal{P} + e\mathbf{A}/c)^2/(m_e c^2)\right]^{1/2}$.

1D case: all the variables that characterize the fields and the plasma are independent of y and z and $A_x = 0$ and $\mathcal{P}_{\rm y} = \mathcal{P}_{\rm z} = 0$.
We can rewrite equations (6)-(8) in components as

$$\partial_{\rm xt}\varphi - 4\pi e n_e p_{||}/m_e c\gamma = 0 \ , \tag{10}$$

$$\partial_{xx}\mathbf{A}_\perp - \partial_{\rm tt}\mathbf{A}_\perp - (4\pi e^2 n_e/m_e c^2\gamma)\mathbf{A}_\perp = 0 \ , \tag{11}$$

$$n_e = n_i(x) + \partial_{xx}\varphi/4\pi e, \tag{12}$$

$$\partial_{\rm t} p_{||} + \partial_{\rm x}(e\varphi - m_e c^2\gamma) = 0, \tag{13}$$

where $\gamma = [1 + (e\mathbf{A}_\perp/m_e c^2)^2 + (p_{||}/m_e c)^2]^{1/2}$.

Subscripts $||$ and $\perp$ denote the components of the vectors along and perpendicular to the x-axis.

Assume homogeneous ion density and wave propagating with constant velocity v_{ph}. Look for solutions that depend on the variable $X = x - v_{ph}t$. We obtain for the electron density

$$n_e = \frac{n_i m_e v_{ph} \gamma}{m_e c \beta_{ph} \gamma - p_{||}}, \tag{14}$$

and the two coupled equations for $\gamma = \gamma(p_{||}, |\mathbf{A}_\perp|)$ and $\mathbf{A}_\perp$

$$(\beta_{ph} p_{||} - m_e c \gamma)'' - \frac{\omega_{pe}^2 p_{||}}{(m_e c \beta_{ph} \gamma - p_{||}) c^2} = 0, \tag{15}$$

$$\mathbf{A}_\perp'' + \frac{\omega_{pe}^2 \beta_{ph} \gamma_{ph}^2}{(\beta_{ph} \gamma - p_{||}) c^2} \mathbf{A}_\perp = 0\,. \tag{16}$$

Here and below $\beta_{ph} = v_{ph}/c$ and $\gamma_{ph} = (1 - \beta_{ph}^2)^{-1/2}$, a prime denotes a differentiation with respect to the variable X.

Longitudinal Relativistically Strong Waves in Cold Plasmas

Assuming the transverse components of electron momentum to be zero which implies $\mathbf{A}_\perp = 0$ and $\gamma = \gamma(p_{||})$, we obtain from equation (15):

$$[(\beta_{ph} p_{||}/m_e c - \gamma)']^2/2 = (\omega_{pe}^2/c^2)\,(\gamma_m - \gamma)\,, \tag{17}$$

where $\gamma_m = [1 + (p_m/m_e c)^2]^{1/2} = 1/(1-\beta_m^2)^{1/2}$ is an integration constant, and $\beta_m c$ the maximum value of the electron velocity in the longitudinal wave: $-\beta_m \le \beta = p_{||}/m_e c\gamma \le \beta_m$. Integrating equation (17) we obtain

$$(2\beta_{ph})^{1/2}(\omega_{pe}/c)X = (\gamma_m - \gamma)^{1/2} - 2\beta_{ph}\left[F\left(\Psi,\kappa\right) - (\gamma_m + 1)E\left(\Psi,\kappa\right)\right], \tag{18}$$

where $F\left(\Psi,\kappa\right)$ and $E\left(\Psi,\kappa\right)$ are the incomplete elliptic integrals of the first and second kind, $\Psi = \mathrm{arcsinh}[(\gamma_m - \gamma)^{1/2}/(\gamma_m + 1)^{1/2}]$ their argument and $\kappa = [(\gamma_m - 1)/(\gamma_m + 1)]^{1/2}$ their modulus.

In a relativistically strong Langmuir wave the electric field depends on the coordinate X through the relationship

$$E = \frac{m_e \omega_{pe} c}{e} \left[2(\gamma_m - \gamma)\right]^{1/2}. \tag{19}$$

The maximum electric field is at the point where $p_{||}(X) = 0$. The expression for γ given by equation (18) is periodic in X. For the wave frequency we get

$$\omega = \pi \omega_{pe} / \left[2\left(K\left(\kappa\right) - (\gamma_m + 1)E\left(\kappa\right)\right)\right], \tag{20}$$

where $K\left(\kappa\right)$ and $E\left(\kappa\right)$ are the complete elliptic integrals.
The wave frequency does not depend on the phase velocity of the wave (cold plasma).

Simple formulae for the frequency: small and large amplitudes of the wave. In the small amplitude case when $p_m \ll 1$, the frequency is

$$\omega = \omega_{pe} \left[1 - 3(p_m/4m_e c)^2\right], \tag{21}$$

which corresponds to the nonlinear shift of the frequency. In the large amplitude case case when $\gamma_m \gg 1$ the frequency is

$$\omega = \pi\omega_{pe}/(\gamma_m^{1/2} 2^{3/2}). \tag{22}$$

Rewriting this expression in terms of the maximum value of the electron momentum, $p_m = m_e c(\gamma_m^2 - 1)^{1/2}$, we obtain that the period of the wave is $T = 2\pi/\omega = 4(p_m/2m_e c)^{1/2}/\omega_{pe}$.

The expression given by equation (14) becomes singular when *the maximum velocity of the electrons in the wave becomes equal to the wave phase velocity*, i.e., when $\gamma = \gamma_{ph} = (1 - \beta_{ph}^2)^{-1/2}$.

This corresponds to the so called **wave breaking**.

Close to the wave-breaking limit when, $c\beta_m \rightarrow v_{ph}$ *the maximum of the electron density tends to infinity while the width of the density spike tends to zero*.

For $c\beta_m = v_{ph}$, from equations (14) and (18) we obtain that the electron density in the spike tends to infinity as $X \rightarrow 0$ as

$$n(X)/n_0 = 2^{1/3}\gamma_m(3\omega_{pe}X/c\beta_m)^{-2/3} + \ldots . \qquad (23)$$

Note the characteristic cusp like pattern $p \propto x^{2/3}$ that appears in phase plane:

$$p_{||}(X)/m_e c \simeq \beta_m \gamma_m [1 - (3\omega_{pe} X/c\beta_m)^{2/3}] + \dots . \tag{24}$$

Integrating the electron density (23) in the neighborhood of the singularity we find that the total number of particles in the density spike is finite.

The wave breaking imposes a constraint on the maximum value of the electric field in the wave:

$$E_m = \frac{m_e \omega_{pe} c}{e} [2(\gamma_{ph} - 1)]^{1/2} \tag{25}$$

which is *the Akhiezer–Polovin limiting electric field*.

Transverse Relativistically Strong Electromagnetic Waves

For a purely transverse electromagnetic wave, from equation (16) with $p_{\|} = 0$ we find that the amplitude of the transverse component of the vector potential $A_\perp$, $\mathbf{A}_\perp = A_y + iA_z = A_\perp \exp(i\omega X/v_{ph})$, is constant and the frequency is

$$\omega = \frac{\omega_{pe}\beta_{ph}\gamma_{ph}}{[1 + (eA_\perp/m_e c^2)^2]^{1/4}}. \tag{26}$$

In the x, t-coordinates this corresponds to the dispersion equation for the frequency and wavenumber

$$\omega^2 = k^2c^2 + \frac{\omega_{pe}^2}{[1 + (eA_\perp/m_e c^2)^2]^{1/2}}. \tag{27}$$

The dispersion equation (27) can be rewritten in the form

$$k = \frac{[\omega^2(1 + (eA_\perp/m_e c^2)^2)^{1/2} - \omega_{pe}^2]^{1/2}}{c[1 + (eA_\perp/m_e c^2)^2]^{1/4}}.$$

The electromagnetic wave can propagate (*relativistic transparency*) in an overdense plasma, where $\omega \ll \omega_{pe}$, provided

$$\omega \gg \omega_{pe}/[1 + (eA_\perp/m_e c^2)^2]^{1/4}. \tag{28}$$

The e.m. fields in the wave are $E = \omega A_\perp/c$ and $B = c\omega A_\perp/v_{ph}$.
The wave velocity is greater than the speed of light in vacuum:

$$v_{ph} = c\,[1 - \omega_{pe}^2/\omega^2(1 + (eA_\perp/m_e c^2)^2)^{1/2}]^{-1/2}. \tag{29}$$

In the case of a purely transverse electromagnetic wave we can also look for the wave-packet solution of equations (10)-(13) in the form $n_e = n_i$, $p_{||} = 0$ and $\mathbf{A}_\perp = A_y + iA_z = A_\perp(x - v_g t)\exp[-i\omega(t - x/v_{ph})]$ with $v_{ph} \neq v_g$.
We obtain

$$\omega = \frac{\omega_{pe}\beta_g\gamma_g}{[1 + (eA_\perp/m_e c^2)^2]^{1/4}} \tag{30}$$

and the relation $v_g v_{ph} = c^2$ for the group and phase velocity.

Langmuir Wave Excitation

Consider a circularly polarized laser pulse with dimensionless amplitude a, propagating in an underdense plasma ($\omega_0 \gg \omega_{pe}$) along the x-axis.
Write the dimensionless vector potential a in the form

$$a(X,t)\exp(-i\omega_0 t - ik_0 x) + c.c..$$

The complex amplitude $a(X,t)$ is a function of the variables t and $X = x - v_g t$ with v_g the group velocity $v_g = c^2 k_0/\omega_0$. Assume the ions to be at rest.
Assume that the change in time of $a(X,t)$ and of the dimensionless electrostatic potential $\phi(X,t)$ are slow ($\partial/\partial t \ll c\partial/\partial X$) and that $v_g \approx c$.
From the relativistic hydrodynamic equations and from Maxwell's equations (6-8) we obtain a system of coupled equations[3]

[3] See e.g., S.V. Bulanov, *et al*, *JETP Lett.* , **50**, 176 (1989);
S. V. Bulanov,*et al*, *Sov. J. Plasma Phys.* **16**, 543 (1990).

$$2i\omega_0\frac{\partial a}{\partial t}+\left(\frac{\omega_{pe}}{\omega_0}\right)^2 c^2\frac{\partial^2 a}{\partial X^2}+2v_g\frac{\partial^2 a}{\partial X\partial t}=\left(\frac{\omega_{pe}}{\omega_0}\right)^2\frac{\phi}{1+\phi}a, \tag{31}$$

$$\frac{\partial^2\phi}{\partial X^2}=\frac{k_p^2}{2}\left[\frac{1+|a|^2}{(1+\phi)^2}-1\right], \tag{32}$$

where $k_p=\omega_{pe}/v_g$.
Here the vector potential a is normalized on $m_e\omega_0 c/e$ and the electrostatic potential ϕ is normalized on $m_e c^2/e$.
If $a=0$, equation (32) describes free Langmuir oscillations in the limit $v_{ph}=c$ considered above (see equation (17)).

If for the sake of reasoning, the laser pulse is assumed to be given as a square-pulse profile with amplitude a_0 ($|a|^2=a_0^2$ at $L<X<0$, and $|a|^2=0$ at $X<L, X>0$), equation (32) can be solved analytically.

In the region occupied by the pulse in terms of elliptic functions we have

$$k_p X = -2(1+a_0^2)^{1/2} E \left\{ \arcsin \left[\left(\frac{(1+a_0^2)\phi}{a_0^2(1+\phi)} \right)^{1/2} \right], \frac{a_0}{(1+a_0^2)^{1/2}} \right\}$$

$$+2 \left(\frac{\phi(a_0^2-\phi)}{1+\phi} \right)^{1/2}. \qquad (33)$$

By matching this solution with the solution for the free plasma wave, we obtain that the typical value of the electrostatic potential in the plasma wave is

$$\varphi_{max} \approx m_e c^2 a_0^2/e. \qquad (34)$$

The optimal pulse length is $L = 2(1+a_0^2)^{1/2} E\left(a_0/(1+a_0^2)^{1/2}\right)$.

The corresponding wake field has a wavelength equal to $\lambda = 2^{3/2}|a_0|k_p^{-1}$, and the maximum electric field (before breaking, it can be higher in a breaking wave) is

$$E = m_e c^2 \omega_{pe} a_0^2/(1+a_0^2)^{1/2} e. \tag{35}$$

The maximum electron energy in the wake wave is given by

$$\frac{1}{2}\left(\frac{d\phi}{dX}\right)^2 = \frac{k_p^2}{2}\frac{\varphi(a_0^2-\phi)}{1+\phi}. \tag{36}$$

Here the constant of integration is chosen such that there is no wake wave before the laser pulse. We see that the potential inside the laser pulse varies between zero and $m_e c^2 a_0^2/e$. Behind the laser pulse, for an optimal pulse length, the electrostatic potential also scales as a_0^2.

In the case of a laser pulse with amplitude $a > (m_i/m_e)^{1/2}$, which corresponds to the petawatt power range, ions can no longer be considered to remain at rest. The modifications of the wake field generated by a sufficiently short laser pulse with $a \approx (m_i/m_e)^{1/2}$ propagating in an underdense plasma (see for comparison equations (15) and (32)) are given by

$$\frac{d^2\phi}{dX^2} = \frac{\gamma_{ph}^3 \beta_{ph} \left(1+\phi\right)}{\left[\gamma_{ph}^2 \left(1+\phi\right)^2 - \left(1+a^2(X)\right)\right]^{1/2}} \tag{37}$$

$$- \frac{\gamma_{ph}^3 \beta_{ph} \left(\mu-\phi\right)}{\left[\gamma_{ph}^2 \left(\mu-\phi\right)^2 - \left(\mu^2+a^2(X)\right)\right]^{1/2}},$$

where $\mu = m_i/m_e$.

We assume the (circularly polarized) laser pulse to be given. The effect of the ion motion restricts the potential ϕ between the two bounds (in these estimates we assume $\beta_g \to 1$)

$$-1 < \phi < \min\{\mu, a_{\rm m}^2\}. \tag{38}$$

From equation (37) we can also find that behind a short laser pulse with optimal length $l = 2^{1/2}/a_{\rm m}$, $\lambda_{\rm w}$ and the maximum value of the electric field $E_{\rm w}$ and of the potential $\phi_{\rm w}$ scale for $1 < a_m < \mu^{1/2}$, as

$$\lambda_{\rm w} = 2^{3/2} a_{\rm m}, \quad E_{\rm w} = a_{\rm m}/2^{1/2}, \quad \phi_{\rm w} = a_{\rm m}^2,$$

and, for $a_m > \mu^{1/2}$, as

$$\lambda_{\rm w} = 2^{1/2}\mu/a_{\rm m}, \quad E_{\rm w} = a_{\rm m}/2^{1/2}, \quad \phi_{\rm w} = \mu$$

For $a_{\rm m} > \mu^{1/2}$ the wake field wavelength decreases with increasing laser pulse amplitude while the value of the electrostatic potential does not change.

Relativistic Solitons

Among nonlinear modes, solitons are of fundamental importance for basic nonlinear science.

Nonlinear one-dimensional (1-D) relativistic solitons have been studied analytically and numerically [4]

Two-dimensional (2D) and 3D subcycle solitons have been found with PIC

[4] N.L. Tsintsadze, D.D. Tskhakaya, *JETP* **45**, 252 (1977);
V.A. Kozlov, A.G. Litvak, and E.V. Suvorov, *Sov. Phys. JETP* **76**, 148 (1979);
R.N. Sudan, Ya.S. Dimant, and O.B. Shiryaev, *Phys. Plasmas* **4**, 1489 (1997)
T.Zh. Esirkepov, F.F. Kamenets, S.V. Bulanov, N.M. Naumova, *JETP Lett.* **68**, 36, (1998).
S.V. Bulanov, T.Zh. Esirkepov, F.F. Kamenets, and N.M. Naumova, *Plasma Phys. Rep.* **21,** 600 (1995);
see recent review D. Farina, S.V. Bulanov, *Plasma Phys. Contr. Fusion*, **47**, A73 (2005).

simulations[5] and "detected" experimentally[6]

Let us return to the relativistic electron equations (6-8), assume the electromagnetic wave to be circularly polarized, introduce the new coordinates $X = x - v_s t$, and $\tau = t$, and look for solutions of the form:

$$\mathbf{A}_\perp = A_\mathrm{y} + iA_\mathrm{z} = A(X)\exp[i\omega((1-v_s^2)\tau - v_s X)], \tag{39}$$

$$p_{||}/m_e c = \beta_s b(X)\,. \tag{40}$$

[5] S. V. Bulanov, T. Zh. Esirkepov, N. M. Naumova, *et al., Phys. Rev. Lett.* **82**, 3440 (1999);
S.V. Bulanov, F. Califano, T.Zh. Esirkepov, *et al., J. Plasma Fusion Research* **75**, 506 (1999);
Y. Sentoku, T.Zh. Esirkepov, K. Mima, *et al., Phys. Rev. Lett.* **83**, 3434 (1999);
N.M. Naumova, *et al., Phys. Rev. Lett.* **87**, 185004 (2001)
T. Esirkepov, K. Nishihara, S.V. Bulanov, F. Pegoraro,*Phys. Rev. Lett.*, **89**, 275002 (2002).

[6] M. Borghesi, *et al., Phys. Rev. Lett.* **88**, 135002 (2002).

Inserting expressions (39,40) into (10-13) and assuming the ion density to be homogeneous we obtain

$$\left(\gamma - \beta_s^2 b\right)'' = \frac{\omega_{pe}^2 b}{(\gamma - b)c^2}, \tag{41}$$

$$A'' + \frac{\omega^2}{c^2}A = \frac{\omega_{pe}^2 \gamma_s^2}{(\gamma - b)c^2}A, \tag{42}$$

where $\gamma = \left(1 + a^2 + \beta_s^2 b^2\right)^{1/2}$, $\gamma_s = \left(1 - \beta_s^2\right)^{-1/2}$, $\beta_s = v_s/c$, $a = eA/m_e c^2$ and a prime denotes a differentiation with respect to the variable X.

The system of equations (41,42), with boundary conditions $a(\infty) = b(\infty) = 0\,,\quad a(X) < \infty\,,\quad b(X) < \infty\,,$ describes a one-dimensional relativistic electromagnetic soliton propagating through a cold collisionless plasma.

The soliton speed and frequency are smaller than the speed of light and of the electron plasma frequency: $\beta_s < 1$ and $\omega < \omega_{pe}$. In the case $v_s = 0$, $p_{||}$ vanishes and we have

$$a'' + k_p^2[(\omega/\omega_{pe})^2 - (1 + k_p^2\gamma'')/\gamma]a = 0\,, \tag{43}$$

where $k_p = \omega_{pe}/c$. With the help of the substitution $a = \mathrm{sh}u$, $\gamma = \mathrm{ch}u$ this equation can be transformed into

$$u'' = k_p^2 \mathrm{sh}\, u\ [1 - (\omega/\omega_{pe})^2\, \mathrm{ch}u]. \tag{44}$$

which gives

$$a(X,\tau) = \frac{2[1-(\omega/\omega_{pe})^2]^{1/2}\ \cosh\left[k_p^2 X\left(1-(\omega/\omega_{pe})^2\right)^{1/2}\right]\exp(i\omega\tau)}{\cosh^2\left[k_p^2 X\left(1-(\omega/\omega_{pe})^2\right)^{1/2}\right] + 1 - (\omega/\omega_{pe})^2}\quad . \tag{45}$$

The relationship between the soliton amplitude $a_{\rm m}$, which is equal to $a_{\rm m} = a(0,0)$, and the soliton frequency ω is given by

$$a_{\rm m} = 2\omega_{pe} \left(\omega_{pe}^2 - \omega^2\right)^{1/2} / \omega^2 \; . \tag{46}$$

Ion motion has important effect on the propagating envelope (multi-humped) solitons and single cycle solitons. It can be shown[7] (in the framework of two fluid cold equations) that no solution can be found for propagation velocities v_s smaller than a critical value $v_{s,cr}$
The non propagating solution given in Eq.(45) is not continuously connected to those with $v_s \neq 0$: its structure will change on the ion dynamical time.

[7] D. Farina, S.V. Bulanov, Phys. Rev. Lett. 86, 5289 (2001);
D. Farina, S.V. Bulanov, Plasma Phys. Rep. 27, 641 (2001)

Electron vortices

Fluid and magnetic vortices represent the final stage of the development of turbulence in plasmas [8].

Electron fluid vortices are indeed produced in the interaction of an ultra short high-intensity laser pulse with an initially unmagnetized plasma [9]

PIC simulations show that finite width and length laser pulses can produce a quasistatic magnetic field[10].

[8] See, e.g., R.L.Stenzel, J.M.Urrutia, and C.L.Rousculp,*Phys. Rev. Lett.* **74**, 702, (1995); W.Horton, and A.Hasegawa, *Chaos*, **4**, 227 (1994).

[9] S.V. Bulanov, T.Zh. Esirkepov, M. Lontano, F. Pegoraro *et al., Phys. Rev. Lett.* **76**, 3562 (1996); S.V. Bulanov, T.Zh. Esirkepov, M. Lontano, F. Pegoraro, *Plasma Phys. Rep.* **23**, 660 (1997).

[10] D.W. Forslund, J.M. Kindel, W.B. Mori, C. Joshi and J.M. Dawson *Phys. Rev. Lett.* **54**, 558, (1985); G.A. Askar'yan, S.V. Bulanov, F. Pegoraro, and A.M. Pukhov, *JETP Lett.* **60**, 241 (1994).

In collisionless plasma regimes this magnetic field is associated to the nonlinear development of the current filamentation instability[11] (which is a Weibel-type[12] instability)

This magnetic field remains behind the pulse and forms a magnetic wake associated with a row of electron fluid vortices which are described by the *Hasegawa-Mima equation*.

Use fluid non relativistic two-dimensional (incompressible[13]) electron equations.

[11] F. Califano, F. Pegoraro, S.V. Bulanov, Phys. Rev.,**E 56**, 963, (1997);
more recently: F. Califano, D. Del Sarto, F. Pegoraro, *Phy. Rev. Lett.*, **96**, 105008 (2006);
M. Tzoufras, *et al. Phy. Rev. Lett.*, **96**, 105002 (2006).

[12] E.W. Weibel, Phys. Rev. Lett., **2**, 83, (1959).

[13] Their motion is slow compared to the Langmuir time and their velocity is much smaller than speed of light c

The z-component of the rotation of the generalized momentum $\nabla \times [\mathbf{p} - (e/c)\mathbf{A}]$ is frozen into the electron fluid.
Then, using $\mathbf{v} = -(c/4\pi en)\nabla \times \mathbf{B}$ with $\mathbf{B}$ to be along z, we obtain

$$\left(\frac{\partial}{\partial t} + \hat{z} \times \nabla B \cdot \nabla\right)(\Delta B - B) = 0, \tag{47}$$

where the time[14] and space[15] units are $\omega_{Be}^{-1} = a^{-1}(\omega/\omega_{pe})^2$ and c/ω_{pe}.
Equation (47) is known as the Charney equation[16] or the Hasegawa-Mima equation in the limit of zero drift velocity[17].

[14] Inverse of the effective cyclotron frequency: the magnitude of the quasistatic magnetic field is estimated to be of order $B_0 \approx a m_e \omega_{pe} c/e$

[15] Electron skin depth which is the characteristic scalelength of the electron vortices

[16] J.G.Charney, *Geophysical Publ*, **17**, 17 (1947)

[17] A. Hasegawa, K. Mima, Phys. Fluids,**21**, 87 (1978).

Discrete vortex model

Eq.(47) has a discrete vortex solution for which the generalized vorticity is localized at the points $\mathbf{r} = \mathbf{r}_j$:

$$\Omega = \Delta B - B = \sum_j \Gamma_j \delta(\mathbf{r} - \mathbf{r_j}(t)), \tag{48}$$

where Γ_j are constants and $\mathbf{r} = (x, y)$. Then we have

$$B = \sum_j B_j, \quad B_j(\mathbf{r}, \mathbf{r}_j(t)) = -(\Gamma_j/2\pi)\ K_0(\mid \mathbf{r} - \mathbf{r_j}(t) \mid), \tag{49}$$

where $K_n(\xi)$ are modified Bessel functions.

The curves $\mathbf{r_j}(t)$ are determined by the characteristics of Eq.(47)

$$\dot{\mathbf{r}}_j = \hat{z} \times \nabla \cdot \sum_{k \neq j} B_k(\mathbf{r}_j(t), \mathbf{r}_k(t)). \tag{50}$$

The equation of motion of the vortices is

$$\dot{x}_j = -\frac{1}{2\pi} \sum_{k \neq j} \Gamma_k \frac{y_j - y_k}{r_{jk}} K_1(r_{jk}), \;\; \dot{y}_j = \frac{1}{2\pi} \sum_{k \neq j} \Gamma_k \frac{x_j - x_k}{r_{jk}} K_1(r_{jk}), \tag{51}$$

where $r_{jk} = \mid \mathbf{r_j} - \mathbf{r_k} \mid = [(x_j - x_k)^2 + (y_j - y_k)^2]^{1/2}$.

Higher dimensions: numerical simulations

These results have been derived using idealized low-dimensionality models. At higher dimensions these investigations are technically and sometimes conceptually (example: topology of field lines in 3D solitons) much more difficult and exact solutions are seldom available.

Numerical simulations play a fundamental role in the analysis of regimes that are outside the reach of most analytical developments because of their high dimensionality and because of their full nonlinear dynamics.

Simulations here are not only used for validating analytical models, but also as an investigative tool for discovering new phenomena. This simulation analysis must be accompanied by the development of an appropriate semantics that can only be obtained from a physical understanding based on the extrapolation of simplified, lower dimensionality, models.

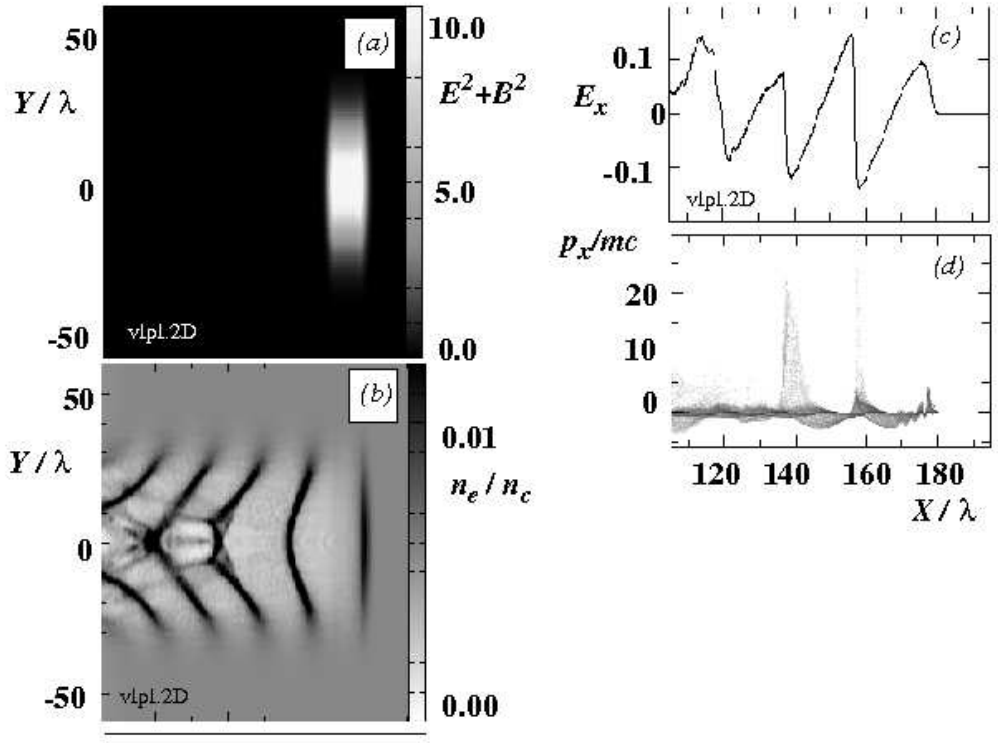

Figure 1: **Wakefield with transverse wave break**, from *S.V. Bulanov, F. Pegoraro, A.M. Pukhov, A.S. Sakharov*, Phys. Rev. Lett., 78, 4205,(1997)

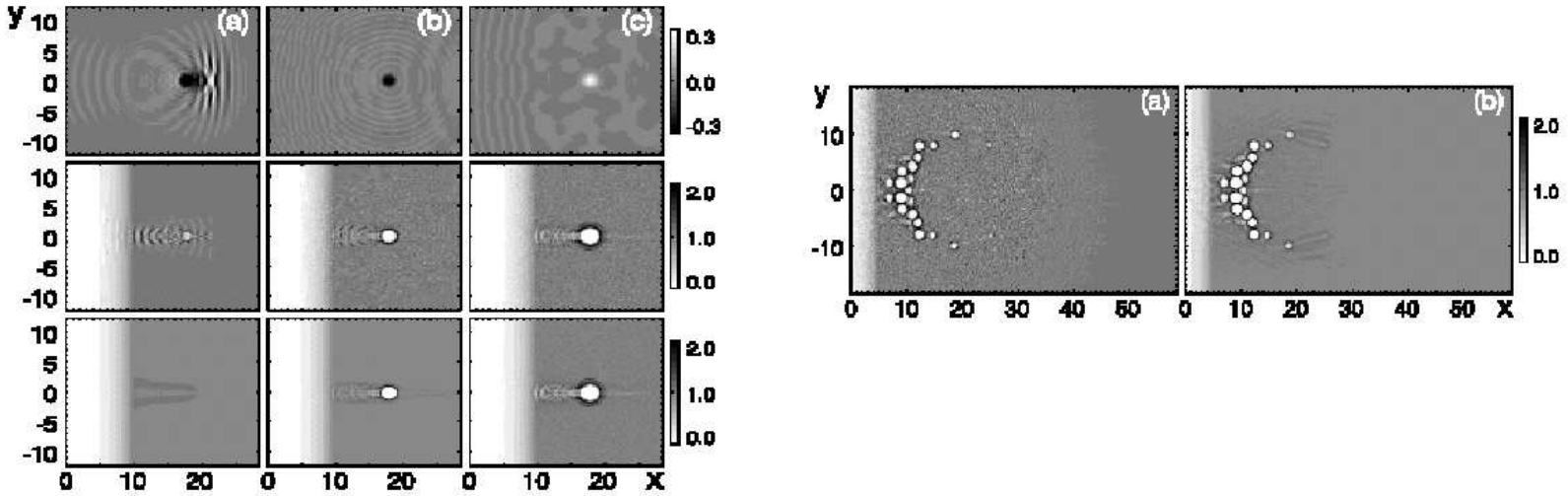

Figure 2: **2D (post)solitons with mobile ions**, from $N.M.\ Naumova$, et al., Phys. Rev. Lett., 87, 185004, (2001)

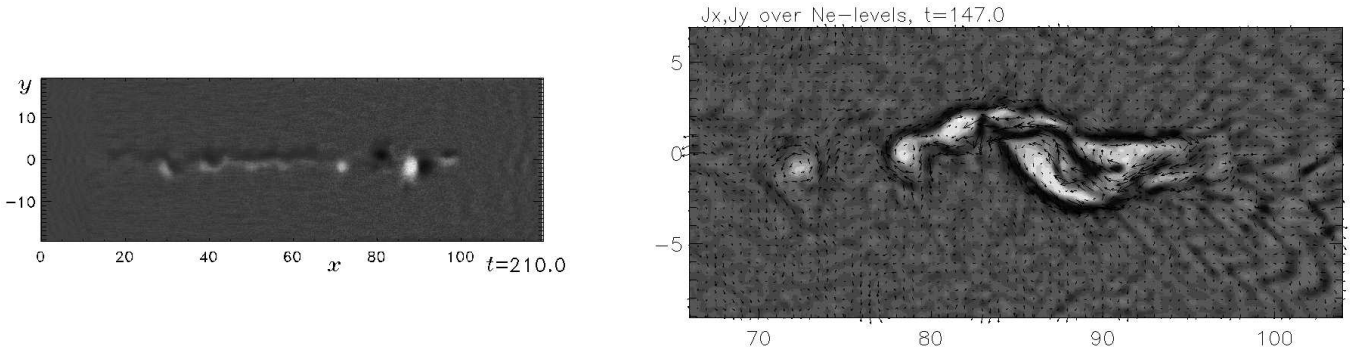

Figure 3: **Kelvin-Helmholtz unstable dipolar magnetic field and electron vortices** , from $N.M.\ Naumova$, et al., Phys. Plasmas, 8, 4149 (2001)

Note: the stronger dipole vortex (located at $x \approx 90$) is asymmetric and moves slowly downwards (also turning around the stronger positive vortex).

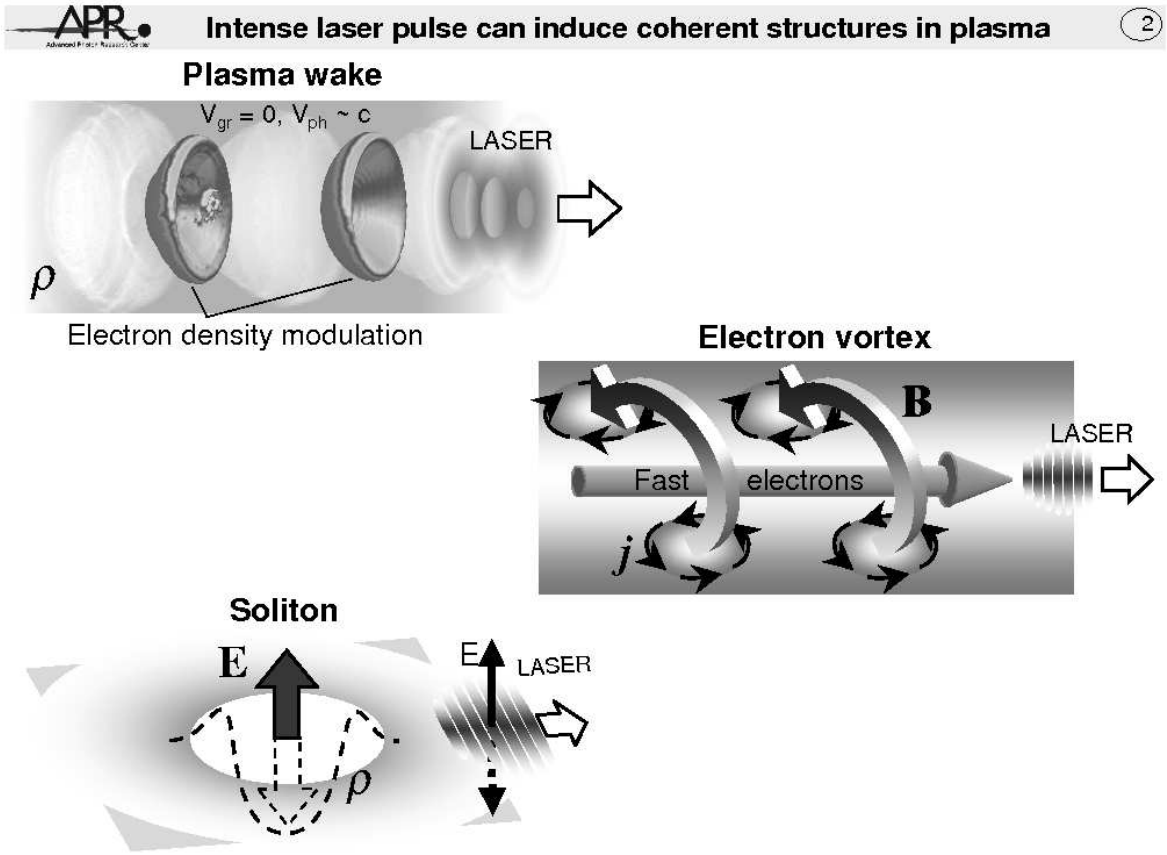

Figure 4: **Schematic summary of the main nonlinear structures**

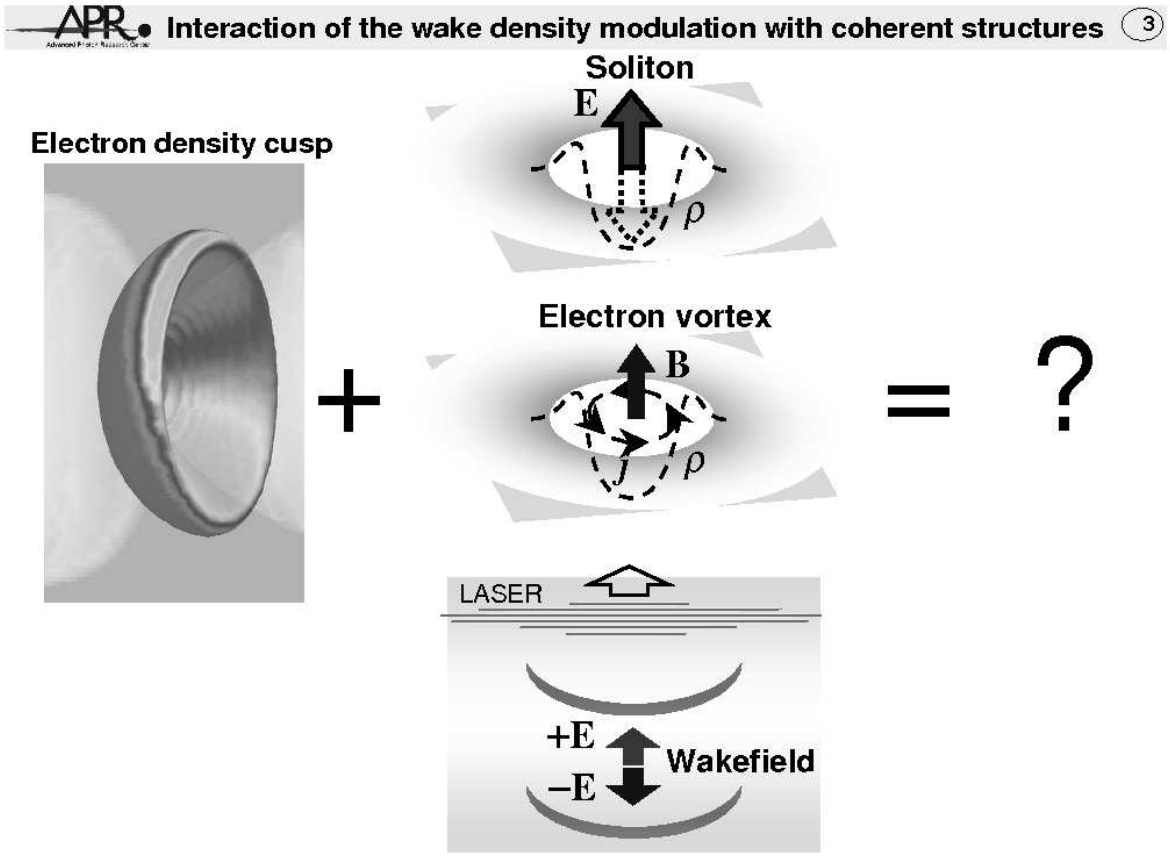

Figure 5: **Reflection processes to be investigated**

Reflection Results: Analytical and Numerical Investigations

In the recent Ref. A.V. Isanin, *et al.*, Phys. Lett. **A 337**, 107 (2005) the mechanism of energy enhancement described in S.V. Bulanov, *et al.*, Phys. Rev. Lett. **91**, 085001 (2003) (where it was shown that when a laser pulse interacts with a breaking wake plasma wave part of the pulse is reflected in the form of a highly compressed and focused e.m. pulse with an up-shifted carrier frequency) was extended to the case where the role of laser pulse is taken by a sub-cycle soliton produced by another laser pulse in the plasma.

These results were confirmed in Ref. S.S. Bulanov, *et al.*, Phys. Rev. E **73**, 036408 (2006) on the basis of two-dimensional (2D) particle-in-cell (PIC) simulations[18] and extended to other types of coherent nonlinear structures: an electron vortex and a wake field.

[18] T.Zh. Esirkepov, Comput. Phys. Comm. **135**, 144 (2001).

One-dimensional analytical model

As already mentioned, the reflection of one-dimensional coherent structures can be derived by performing a Lorentz transformation to the reference frame where the wake plasma wave is at rest. In this frame the e.m. fields are Fourier transformed with respect to time and the frequency dependent reflection coefficient

$$\rho(\omega') = -q/(q - i\omega'), \tag{52}$$

where $q = 2\omega_{pe}(2\gamma_{ph})^{1/2}$ is used and γ_{ph} is the Lorentz factor corresponding to the phase velocity of the wake wave[19]

The form and amplitude of the reflected pulse in the laboratory frame can obtained by adding the reflected Fourier components and by performing the inverse Lorentz transformation of the resulting e.m. fields.

[19] In this model the mirror is taken not to be deformed by the interaction with the coherent structure in a sort of "test particle approach" where the energy of the mirror, of the wake wave that produces it, is as large as required.

The main conclusion of this one dimensional analysis is that

• *the amplitudes of the e.m. fields in the reflected pulse are increased by the factor* $\gamma_{ph}^{3/2}$,

• • *i. e., the pulse intensity is proportional to* γ_{ph}^{3},

• • • *while its frequency is up-shifted by* $2\gamma_{ph}^{2}$.

This scaling indicates that in a tenuous plasma the frequency up-shift of the reflected pulse, and its related compression, would be so large that it could lead to the generation of attosecond pulses.

To take into account the effects of multi-dimensional geometry and strongly nonlinear plasma dynamics, as well as the influence of kinetic effects, two dimensional simulations were performed.

Numerical documentation

The grid mesh size is $\lambda_d/20$; space and time unit is λ_d and $2\pi/\omega_d$, respectively. Here λ_d and ω_d is the driver laser wavelength and frequency, respectively.
The electric and magnetic field components are normalized to $m_e\omega_d c/e$ and the electron density is normalized to the critical density $n_{cr} = m_e\omega_d^2/4\pi e^2$.
The ions are assumed to form an immobile neutralizing background and thus only the electron motion is taken into account. This approximation is applicable because the typical interaction period is much shorter than the ion response time.
The boundary conditions are absorbing for the e. m. field and the quasi-particles.

The interaction of a wake wave with a soliton is simulated in a box with size $60\lambda_d \times 40\lambda_d$, including the absorbing edges of thickness $3\lambda_d$.
A single relativistic e. m. sub-cycle soliton is generated by an auxiliary laser pulse with wavelength $\lambda_a = 2\lambda_d$ and dimensionless amplitude $a_a = 0.5$, corresponding to the peak intensity $a_a^2 \times I_1$, where $I_1 = 1.37 \times 10^{18}$ W/cm$^2 \times (1\ \mu m/\lambda_d^2)$.
The pulse is Gaussian with FWHM size (length×waist) $4\lambda_d \times 6\lambda_d$.
The auxiliary laser pulse is linearly polarized with its electric field along the z-axis; it is generated at the bottom boundary at $t = 0$ and propagates along the y-axis at $x = 20$.
The plasma wakefield, which interacts with the soliton, is formed by a Gaussian laser pulse, the driver pulse, with amplitude $a_d = 1.5$ and FWHM size $2\lambda_d \times 12\lambda_d$, starting at time $t = 45$ from the left boundary and propagating along the x-axis.
The driver laser pulse is linearly polarized, its electric field is directed along the y-axis.

The plasma slab occupies the region $5 \leq x \leq 35$, $5 \leq y \leq 35$; it is homogeneous in the direction of the y-axis and it has convex parabolic slopes along the x-axis from $x = 5$ to 11 and from 29 to 35.
This plasma-vacuum interface profile is chosen so as to make the laser pulse entrance into the plasma smoother and to avoid a fast wake wave breaking.
The electron density at the center of the plasma slab is $n_e = 0.09 n_{cr}$, corresponding to the Langmuir frequency $\omega_{pe} = 0.3$.

The number of quasi-particles is 3.24×10^6.

The phase velocity of the wakefield when it starts to interact with the soliton is $v_{ph} \approx 0.925$, corresponding to the Lorentz factor $\gamma_{ph} \approx 2.63$.

Wake ⊕ Soliton

7

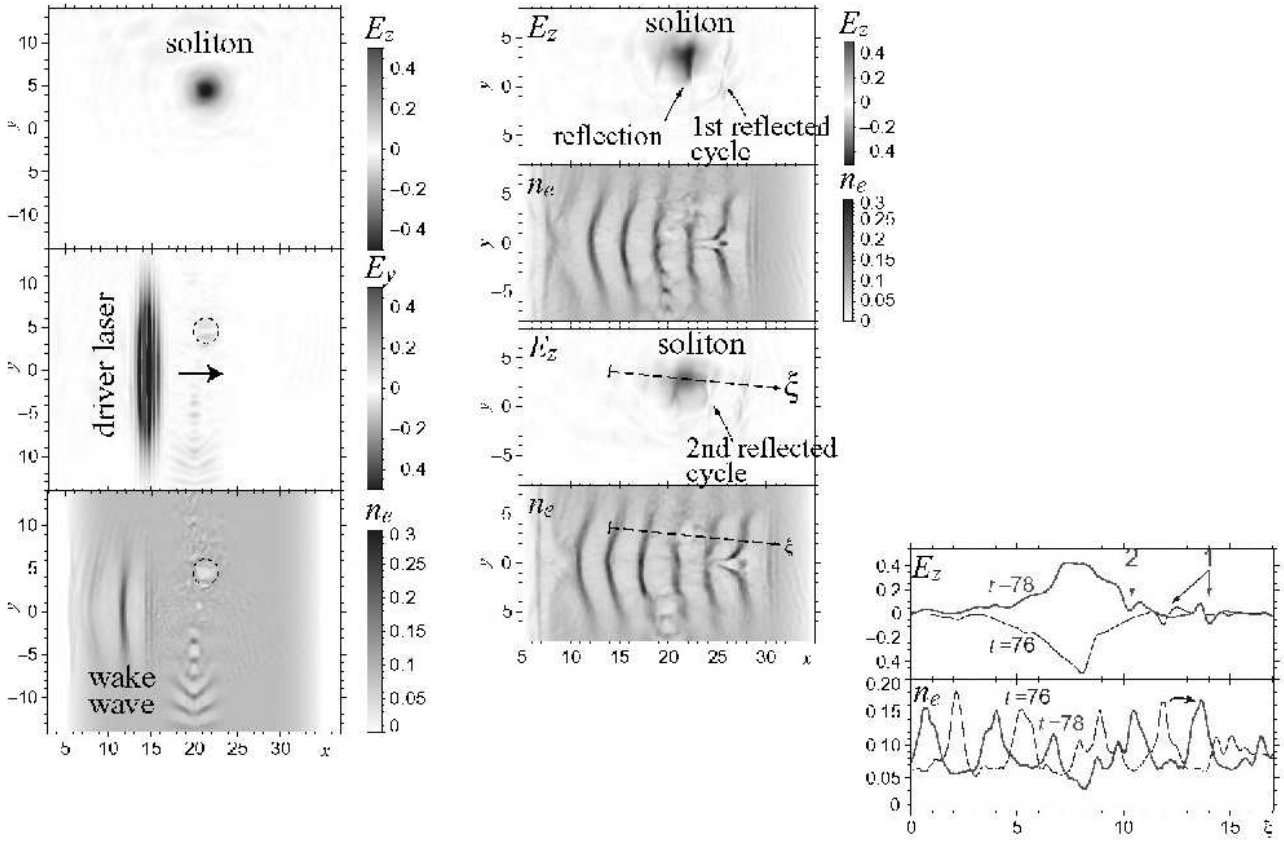

Fig.6 (left) shows a portion of the simulation box shortly before the interaction.

The auxiliary laser pulse has already gone through: in its wake we see a single s-polarized relativistic e. m. sub-cycle soliton and remnants of a broken wakefield at the bottom of the window. The soliton frequency is well below the unperturbed plasma frequency, $\Omega_S \approx 0.25\omega_d < \omega_{pe}$. The soliton appears as a region of low electron density. Since the driver and the auxiliary laser pulses have different polarizations and the soliton inherits its polarization from the auxiliary laser, it is easy to distinguish the e. m. field reflected from the soliton in the distribution of the E_z component. The driver laser pulse induces a strong wakefield which is seen in the electron density distribution as a series of wide regions of rarefaction alternating with thin horseshoe-shaped regions of compression.
Regions of compression correspond to spikes (cusps) in the longitudinal profile of the electron density.

Fig.6 (right) shows the interaction of the density cusps in the wake of the driver pulse with the soliton.

The z-component of electric field and the electron density are shown. The wake wave of the driver is close to the wave breaking regime.
Each electron density maximum (each cusp) in the wake acts as a fast moving semitransparent parabolic mirror that partially reflects the e. m. fields of the soliton as it propagates through the soliton.
The process is repeated when the subsequent cusps of the electron density propagate through the soliton. Thus a set of short e. m. pulses is formed.
Even though the electron density cusp is substantially distorted as it moves through the soliton, it recovers after leaving the soliton. This transient distortion of the cusp when crossing the soliton does not prevent the formation of well pronounced single-cycle pulses.

We also note that the single cycle pulses move faster than the electron ridge. *The frequency of the fields in the reflected single-cycle e. m. pulses is up-shifted and their longitudinal size is much smaller than the size of the soliton.*

Since the soliton is not exactly positioned at the crossing of laser pulse axes, the reflected pulse is not exactly directed along the x-axis.
This is a consequence of the parabolic profile of the wakefield: as the pulse is reflected by the upper wing of parabola it propagates at an angle with respect to the x-axis.

The interaction of a wake wave with an electron vortex, associated with a quasi-stationary transverse magnetic field, is simulated in a box with size $50\lambda_d \times 80\lambda_d$, including absorbing edges of thickness $2\lambda_d$.
The electron vortex is prepared by introducing a magnetic field B_z which increases gradually from $t = 0$ to $t = 10$.
After $t = 10$, a self-consistent quasi-stationary electron fluid vortex is formed with its corresponding magnetic field distribution $B_z = 0.066 \exp\big(- (x - 20)^2/4 - y^2/4\big)$.
The shape of the plasma slab is the same as in the previous simulation except that its transverse size (along the y-axis) is $70\lambda_d$ and the maximum electron density is $n_e = 0.04 n_{cr}$.

The number of quasi-particles is 3.4×10^6.

A Gaussian, linearly polarized (E in the z-direction), driver laser pulse with amplitude $a_d = 1.2$ and FWHM size $2\lambda_d \times 30\lambda_d$, starts from $t = 10$ from the left boundary, propagates along the x-axis, and induces a plasma wakefield which interacts with the electron vortex.
The phase velocity of the wakefield is $v_{ph} \approx 0.965$, so that the Lorentz factor is $\gamma_{ph} \approx 3.81$.
A large waist of the driver laser pulse is chosen to make the interpretation of the reflection easier.

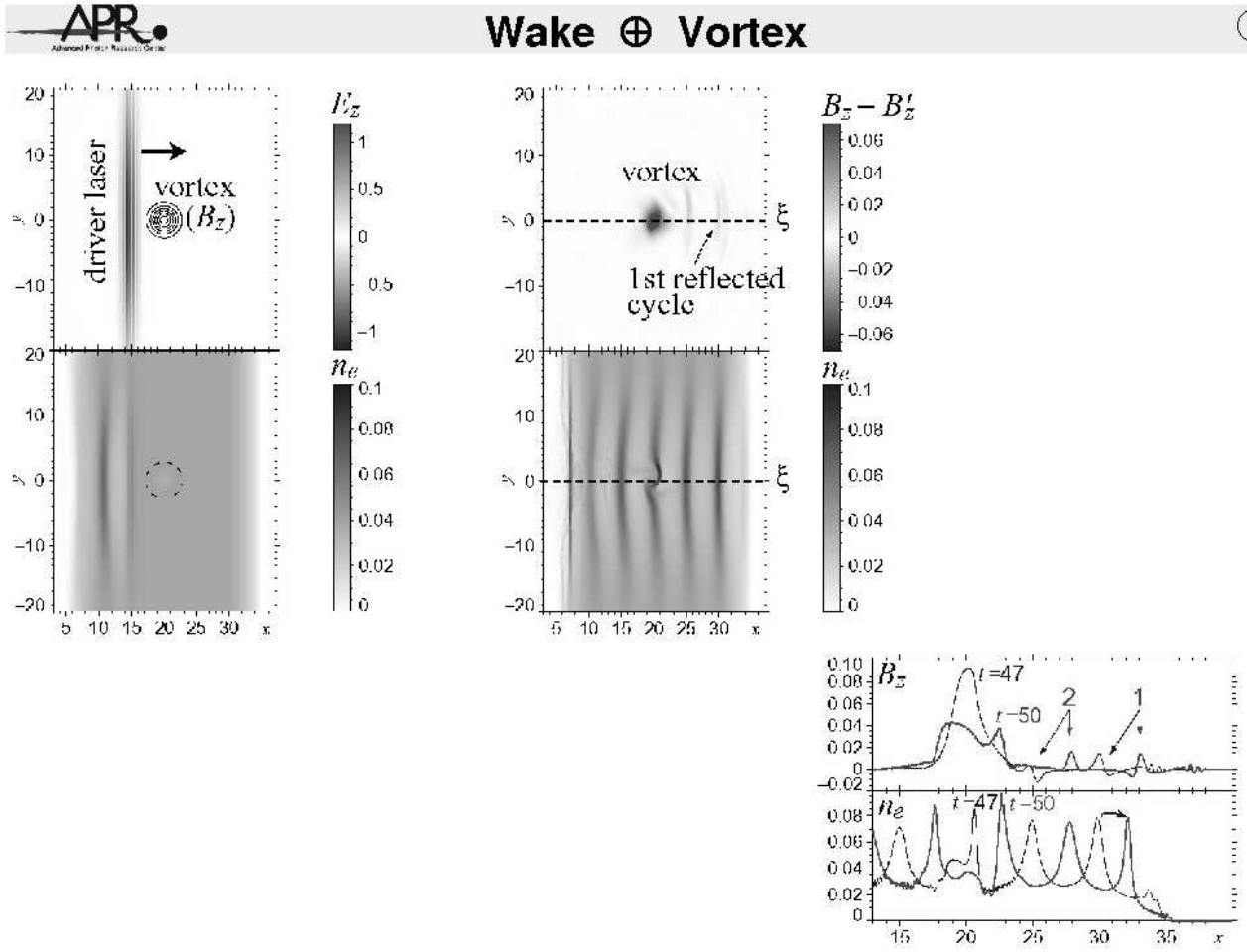
APR
Wake ⊕ Vortex
10
driver laser
vortex
(B_z)
E_z
n_e
vortex
1st reflected
cycle
$B_z - B_z'$
n_e
B_z
t=47
t=50
2
1
n_e
t=47
t=50

Fig.7 shows the z-component of magnetic field[20] and the electron density during the interaction with the vortex.

As in the case of the interaction of the wake wave and a soliton, the electron density cusp is substantially distorted as it moves through the vortex and it recovers after passing the vortex. As in the soliton case this transient distortion of the cusp does not affect the shape of the resulting single-cycle pulses.
We also note that the electron vortex is distorted due to modulations of the electron density in the wake wave.

[20] The wake wave itself has a transverse magnetic field B'_z which arises due to the wake wave curvature. Although the magnetic field of the wake wave does not prevent us from distinguishing the e. m. pulses reflected from the vortex easily, nevertheless, we show the quantity $B_z - B'_z$, where B_z and B'_z are the magnetic field components seen, respectively, in two simulations – one, as described in this section, and the other performed with the same parameters but without the vortex (i. e., with no initial magnetic field). Thus a "pure" reflection of the e. m. field of the vortex, resulting in formation of single-cycle pulses, can be seen.

In order to show the interaction of a wake wave with another (weak) wake wave, we performed a simulation with the same simulation box and plasma distribution as in the previous cases except for the maximum electron density which is now $n_e = 0.01 n_{cr}$.

Two laser pulses, which are linearly polarized (E along the z-axis) and propagate in perpendicular directions, induce two plasma wakes.
The first, auxiliary, laser pulse with Gaussian shape, amplitude $a_a = 0.7$, wavelength $\lambda_a = \lambda_d$ and FWHM size (length$\times$waist) $2.5\lambda_d \times 10\lambda_d$, starts at $t = 0$ from the bottom boundary, propagates in the direction of the y-axis at $x = 20$ and induces a weak wakefield with a longitudinal electric field directed along the y-axis.

The second laser pulse (driver) is switched on at $t = 70$ on the left boundary. Its amplitude is $a_d = 2$ and size is $2\lambda_d \times 50\lambda_d$. The driver pulse has a Gaussian profile in the direction of the x axis; along the y-axis its shape is a smooth centrosymmetric, piecewise polynomial with sizes of adjacent parts $8, 34, 8$. The central part is constant; the profile of the first slope is defined by $(3 - 2\eta)\eta^2$, $\eta = y/8$.

We chose such a shape for the driver laser pulse so as to ensure the transverse homogeneity of the induced wakefield in the region $-17 < y < 17$, and thus to obtain a plasma wake with zero transverse electric field in this region.

With such a configuration, in the distribution of the E_y component inside the region $-17 < y < 17$, we see, in principle, only the electric field of the weak wakefield, induced by the auxiliary laser pulse.

The wakefield from the driver has phase velocity $v_{ph} \approx 0.982$ and the Lorentz factor $\gamma_{ph} \approx 5.32$.

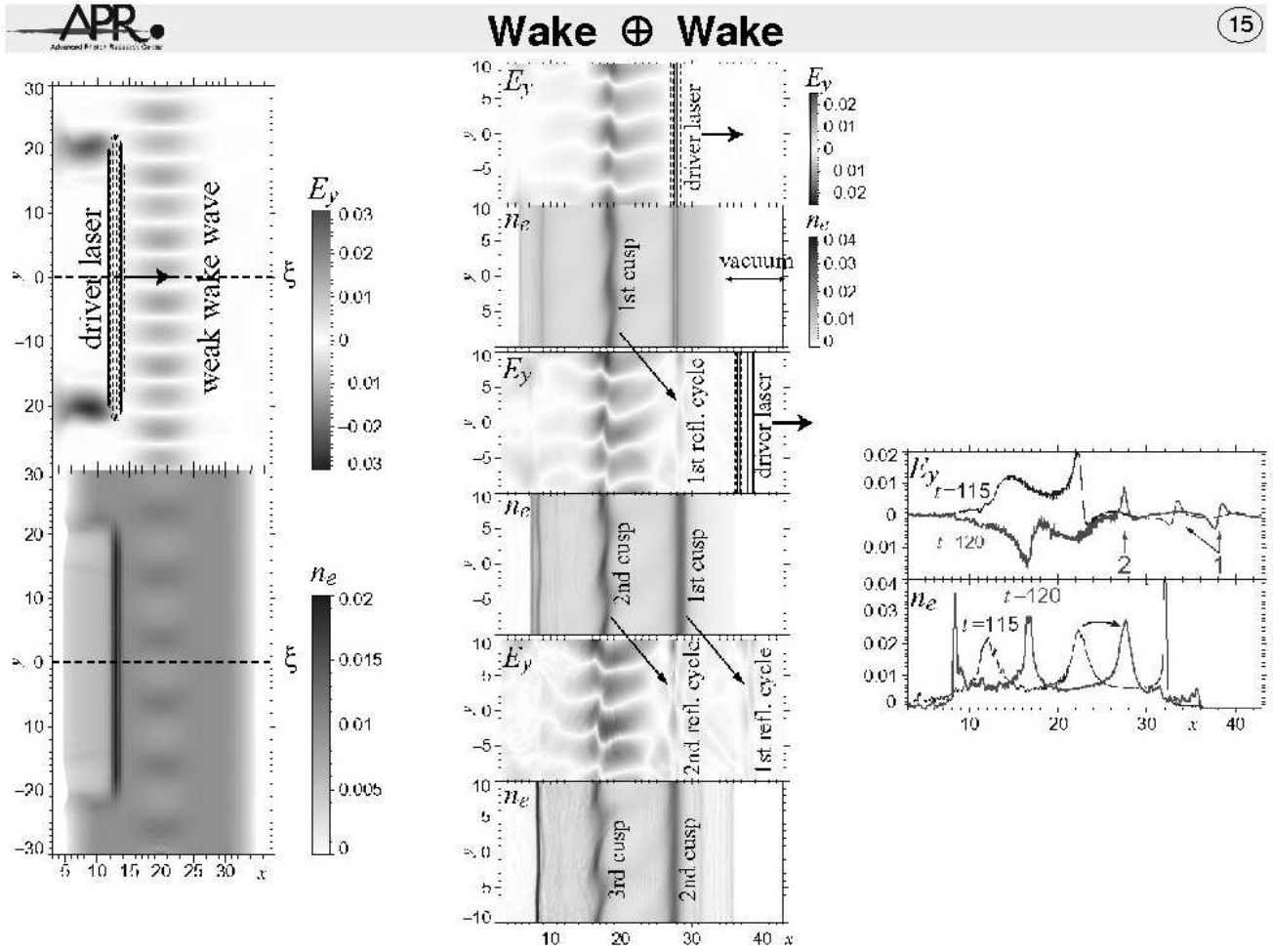
APR
Wake ⊕ Wake
15
driver laser
weak wake wave
E_y
n_e
vacuum
1st cusp
2nd cusp
3rd cusp
1st refl. cycle
2nd refl. cycle
driver laser
$t-115$
$t-120$
$t=115$
1
2

Fig.8 shows the y-component of electric field and electron density at three moments of time with period approximately equal to the period of the plasma wake wave induced by the driver laser pulse. The driver is represented by contours of the z-component of electric field.

As in the case of the interaction of the wake wave with a soliton and vortex, the electron density cusp is distorted inside the weak wake wave, but is almost restored when it moves outside. Even though the electron density cusp seems curved when it is under the influence of the weak wake wave, the single-cycle pulse reflected by this cusp appears to be flat.
As in the cases of other nonlinear coherent structures described above, each density cusp reflects single-cycle e. m. pulse whose frequency is up-shifted and whose intensity is increased due to Doppler effect[21].

[21] A complication, which is not included in the presented 1D theory, arises from the fact that the weak wake wave, which is (partially) reflected by the "mirrors" of the wake from the driver, has almost the same phase velocity as these mirrors.

We also note that ultrashort e. m. pulses can be generated when a wake wave interacts with plasma in a self-focusing channel. In a self-focusing channel, an electric field is present due to charge separation and can be transformed into an ultrashort e. m. pulse, similarly to the soliton, vortex or wake wave.

In conclusion, the reflection of coherent structures by a wake wave can be exploited in order to produce ultra-short intense e.m. pulses with presently available lasers. The modulations of electron density in a strong wake wave close to the wave-breaking regime have the shape of spikes and each spike acts as a semi-transparent mirror moving with a relativistic velocity. Such a mirror partially reflects the electromagnetic field of a coherent nonlinear structure and thus generates an electromagnetic pulse. For each spike, the reflected pulse consists of a single cycle oscillation, which results in a train of single oscillation pulses.